

# Multiple populations of H $\beta$ emission line stars in the Large Magellanic Cloud cluster NGC 1971

Andrés E. Piatti<sup>1,2\*</sup>

<sup>1</sup> Instituto Interdisciplinario de Ciencias Básicas (ICB), CONICET-UNCUYO, Padre J. Contreras 1300, M5502JMA, Mendoza, Argentina;

<sup>2</sup> Consejo Nacional de Investigaciones Científicas y Técnicas (CONICET), Godoy Cruz 2290, C1425FQB, Buenos Aires, Argentina

Received / Accepted

## ABSTRACT

We revisited the young Large Magellanic Cloud star cluster NGC 1971 with the aim of providing additional clues to our understanding of its observed extended Main Sequence turnoff (eMSTO), a feature common seen in young stars clusters, which was recently argued to be caused by a real age spread similar to the cluster age ( $\sim 160$  Myr). We combined accurate Washington and Strömgren photometry of high membership probability stars to explore the nature of such an eMSTO. From different *ad hoc* defined pseudo colors we found that bluer and redder stars distributed throughout the eMSTO do not show any inhomogeneities of light and heavy-element abundances. These 'blue' and 'red' stars split into two clearly different groups only when the Washington  $M$  magnitudes are employed, which delimites the number of spectral features responsible for the appearance of the eMSTO. We speculate that Be stars populate the eMSTO of NGC 1971 because: i) H $\beta$  contributes to the  $M$  passband; ii) H $\beta$  emissions are common features of Be stars and; iii) Washington  $M$  and  $T_1$  magnitudes show a tight correlation; the latter measuring the observed contribution of H $\alpha$  emission line in Be stars, which in turn correlates with H $\beta$  emissions. As far as we are aware, this is the first observational result pointing to H $\beta$  emissions as the origin of eMSTOs observed in young star clusters. The presence outcome will certainly open new possibilities of studying eMSTO from photometric systems with passbands centered at features commonly seen in Be stars.

**Key words.** techniques: photometric – galaxies: individual: LMC – galaxies: star clusters: general – galaxies: star clusters: individual: NGC 1971.

## 1. Introduction

Piatti & Cole (2017) detected an extended Main Sequence Turnoff (eMSTO) in the young Large Magellanic Cloud (LMC) cluster NGC 1971 ( $\sim 160$  Myr) using broadband Washington  $CT_1$  photometry (Canterna 1976). After considering photometric uncertainties, presence of binary stars, variations in the overall metallicity and stellar rotation effects, they concluded that the observed eMSTO could have been caused by a real age spread of  $\sim 170$  Myr, in addition to the above sources of color dispersion in the cluster color-magnitude diagram (CMD). Because H $\alpha$  contributes to the Washington  $T_1$  passband, the broadness of the  $C - T_1$  color range in the NGC 1971's CMD could be due to the presence of Be stars, so that the eMSTO would have its origin in two populations of slow and fast rotators, respectively. However, the  $M$  vs  $C - M$  CMD in Piatti & Cole (2017, see their figure 4) still shows an eMSTO, thus giving support to the idea of a real age spread. eMSTOs have been commonly seen in star clusters with ages similar to that of NGC 1971, including Magellanic Cloud star clusters (e.g., D'Antona et al. 2017; Milone et al. 2017, 2018; Goudfrooij et al. 2018) and Galactic open clusters (Marino et al. 2018a; Cordoni et al. 2018).

In recent years, stellar rotation has been suggested as a main source for the occurrence of the eMSTO phenomenon in young star clusters. Bastian et al. (2017) found a high fraction of Be stars in the LMC clusters NGC 1850 ( $\sim 80$  Myr) and NGC 1856 ( $\sim 280$  Myr) that implies a high fraction of rapidly rotating stars.

These Be stars are located toward the redder end of the cluster eMSTOs (see, also Milone et al. 2018). Dupree et al. (2017) provided with the first spectroscopic evidence that two populations coexist in the LMC cluster NGC 1866 ( $\sim 200$  Myr), consisting in one younger and slowly rotating and another rapidly rotating groups of stars (see, also Gossage et al. 2019). The latter exhibit H $\alpha$  emission lines. Additional spectroscopic evidence is shown by Marino et al. (2018a, see, figure 2) and Marino et al. (2018b, see, figure 8). We note also that the effects of braking in main sequence stars could mimic an age spread (D'Antona et al. 2017).

In this work, we revisited NGC 1971 with the aim of providing additional evidence on the possible origin of its eMSTO. In Section 2 we present Strömgren photometry (Crawford & Mandwewala 1976) for the cluster field, while in Section 3 we analyze light-element abundance variations – usually associated to the existence of multiple populations in globular clusters (Marino et al. 2019) – and show that the presence of Be stars with H $\beta$  emission could have contributed to the  $M$  Washington passband and hence to the spread in the  $C - M$  color. We note that Be stars in eMSTO clusters have been detected from their emission in H $\alpha$ , no evidence for other emission features have been reported. Finally, in Section 4 we summarize the main conclusions of this work.

\* e-mail: andres.piatti@unc.edu.ar

## 2. Strömgren photometric data

We searched the National Optical Astronomy Observatory (NOAO) Science Data Management (SDM) Archives<sup>1</sup> looking for unexploited images in the field of NGC 1971. The observing program SO2008B-0917 (PI: Pietrzyński), carried out with the SOAR Optical Imager (SOI) attached to the 4.1m Southern Astrophysical Research (SOAR) telescope (FOV =  $5.25' \times 5.25'$ , scale =  $0.154''/\text{px}$  in binned mode), obtained Strömgren  $vby$  images centered on the cluster during the night of January 18, 2009 under excellent image quality conditions (typical FWHM  $\sim 0.6''$ ). They consist in  $3 \times 400$  sec,  $3 \times 180$  sec, and  $3 \times 100$  sec exposures in the  $v, b, y$  passbands, respectively, at airmass between 1.42 and 1.50. Standard stars were also observed during the night, namely: HD64, HD3417, HD12756, HD22610, HD57568, HD58489, TYC 7583-1622-1, and TYC 8104-969-1 (Hauck & Mermilliod 1998; Paunzen 2015). They were observed twice at a fixed airmass to allow them to be placed in the two different CCDs arrayed by SOI, and thus to monitor their individual responses. We also downloaded calibration frames (zeros, sky- and dome-flats). We processed the images following the SOI's reduction recipes available at <http://www.ctio.noao.edu/soar/content/soar-optical-imager-soi>. The LMC cluster NGC 1978 was also observed during the same night, so that we took advantage of the transformation equations fitted by Piatti & Bailin (2019), who showed that magnitudes of standard stars placed in each CCD are indistinguishable.

The image processing packages DAOPHOT, ALLSTAR, DAOMATCH and DAOMASTER (stand-alone version, Stetson et al. 1990) were employed to obtain point-spread-function (PSF) magnitudes and their associated uncertainties. We started by selecting interactively nearly one hundred relatively bright, not-saturated and well-isolated stars located throughout the whole image area to construct the corresponding PSF. A nearly 40% of the selected PSF stars were initially chosen to build a preliminary PSF, which was applied to the image in order to clean the whole sample of PSF stars from fainter neighbors. We built the final quadratically spatially-varying PSF for that image from that cleaned PSF star sample, and computed aperture corrections that resulted in the range  $-0.04$  -  $-0.07$  mag. We obtained PSF magnitudes for the entire list of sources identified in the image by applying the respective PSF. From the resulting subtracted image, we identified new sources, which were added to the previous list to obtain simultaneously new magnitudes. We enlarged the list of sources by iterating this procedure three times. With the aim of dealing with stellar sources we only kept those with  $\chi < 2$  and  $|\text{SHARP}| < 0.5$ . As for the mean magnitudes and their uncertainties we straightforwardly averaged the magnitudes measured from the three images collected per passband. Errors were estimated from extensive artificial star tests as previously performed for other subsets of Magellanic Cloud clusters imaged during the same observing program (Piatti & Koch 2018; Piatti 2018; Piatti & Bailin 2019; Piatti et al. 2019; Piatti 2020).

We followed the procedure applied by Piatti & Cole (2017) to clean the cluster CMDs  $V$  vs.  $b-y$  and  $V$  vs.  $m_1$ <sup>2</sup> from field star contamination (Piatti & Bica 2012). The method relies on the use of each pair of magnitude and color in a reference field star CMD to subtract the closest star in the cluster CMD. In doing this, we considered the uncertainties in magnitudes and colors by repeating the procedure hundreds of times with magnitudes and colors varying within their respective errors. We used as ref-

erence fields four different regions with areas equal to the cluster region, which was delimited by a radius of 20 arcsec from the cluster center. In the end, we subtracted a number of stars from the cluster CMD equal to that in each reference field star CMD. From the four resulting cleaned cluster CMDs we assigned membership probabilities to each stars based on the number of times they were subtracted in the four cleaning procedures (one per reference field CMD). For instance, stars that appear in all the cleaned CMDs have a membership probability  $P = 100\%$ , while those seen in three cleaned CMDs,  $P = 75\%$ . We tried to complement our membership probability assignments with kinematical information from the *Gaia* DR2 database (Gaia Collaboration et al. 2016, 2018). Unfortunately, the relatively small and crowded cluster field and its relatively low brightness made in practice unfeasible any accurate measurement of proper motion and parallax of cluster stars. We barely got a ten of stars located within the cluster radius with very distinct proper motion values.

The Washington  $CMT_1$  photometry published by Piatti & Cole (2017) was cross-matched with the present Strömgren photometry, and a master table that included the membership probabilities assigned independently from these data sets was built. In the subsequent analysis, we did not use the  $T_1$  magnitudes, which could be affected by contributions from  $H\alpha$  emission lines, so that the hypothesis of the presence of slow and fast rotators as sources of the eMSTO was avoided from our analysis. Nevertheless, the combination of the Washington  $CM$  and Strömgren  $vby$  magnitudes allowed us to play with different pseudo colors [ $\equiv (m_1 - m_2) - (m_2 - m_3)$ ], with  $m_1, m_2, m_3$  being three different magnitudes] to uncover possible trails of the observed eMSTO in NGC 1971. We refer the reader to Monelli et al. (2013) and Milone et al. (2017) for the definition and usefulness of pseudo colors in the context of multiple population analyses.

## 3. Analysis and discussion

Piatti & Cole (2017) showed that theoretical isochrones for the cluster age and overall metallicities between  $[\text{Fe}/\text{H}] = -0.6$  and  $+0.1$  dex (the cluster metallicity is  $[\text{Fe}/\text{H}] = -0.3$  dex (Dieball & Grebel 2000)) do not account for the observed eMSTO. However, light-element abundance variations were not sought. Indeed, the Washington  $C$  and Strömgren  $v$  magnitudes could reflect CN/CH variations (Cummings et al. 2017; Lim et al. 2017). The  $C$  and  $v$  passbands have effective wavelengths (and FWHMs) at  $\lambda 3910\text{\AA}$  ( $1100\text{\AA}$ ) and  $\lambda 416\text{\AA}$  ( $190\text{\AA}$ ), respectively, so that both include the CN absorption band at  $\lambda 4142\text{\AA}$ ; the  $C$  passband also includes the violet CN bands at  $\lambda 3595\text{\AA}$  and  $\lambda 3883\text{\AA}$ . We note that the  $M$  bandpass ( $\lambda 5058\text{\AA}$  ( $1050\text{\AA}$ )) is freed from CN absorption bands. Figure 1 shows the  $C$  vs.  $(C - v) - (v - M)$  diagram where we highlighted with blue and red filled circles stars that belong to the eMSTO, distributed from the top of the cluster MS down to one magnitude underneath, and with  $(C - v) - (v - M)$  values higher and lower than  $-0.20$  mag, respectively. These stars have membership probabilities  $\geq 75\%$  in the Washington and Strömgren data sets, respectively.

The Strömgren  $m_1$  index is known as an iron abundance sensitive index (Calamida et al. 2007), which also measures variations in light-elements. Therefore, it might reflect both heavy and light-element abundances or only those from light-elements. Because metallicity variations were not found by Piatti & Cole (2017), we concluded that any distinction in the  $m_1$  values between blue and red stars could be caused by different CN/CH abundances, which in turn would imply the existence of two dif-

<sup>1</sup> <http://www.noao.edu/sdm/archives.php>.

<sup>2</sup>  $m_1 = (v - b) - (b - y)$

ferent populations among the stars in NGC 1971. Figure 2 depicts the  $m_1$  vs.  $v - y$  diagram for all the measured stars in Figure 1. It reveals that the two groups of stars selected from Figure 1 do not exhibit any visible separation. There is a couple of stars that remarkably separate from the region where most of the blue and red ones are concentrated. These stars could have anomalous chemical compositions, somehow defective Strömgren photometric data, or be interlopers. Hence, Figure 2 suggests that NGC 1971 harbors stars with similar light-element abundances. Blue and red stars also overlap in any color-color diagram that involves  $b - y$ ,  $v - y$  or  $m_1$ , which means that the Strömgren indices reveal a single population young cluster with an homogeneous chemical abundance distribution. The above results are expected for young star clusters, because MSTO stars have higher temperatures as compared to those of old globular cluster stars. In old globular clusters the magnitude differences between CN-rich and CN-poor stars with similar luminosities are mostly due to the different strengths of molecules including light elements such as C, N or O (e.g., Marino et al. 2008; Yong et al. 2008; Sbordone et al. 2010). In hotter stars such differences are small, and are unlikely consistent with the large color difference between red and blue stars.

Figure 3 depicts the  $(C - v) - (v - M)$  vs.  $C - M$  diagram where the two groups of stars selected from Figure 1 are clearly differentiated. On the assumption that the Washington-Strömgren metallicity sensitive passbands ( $C, v$ ) are not measuring any difference between blue and red stars, we concluded that the distinction between both groups is caused by the Washington  $M$  magnitudes. Indeed, it enters with a different sign in the ordinate and abscissa of Figure 3. Moreover, we would arrive to the same conclusion by comparing, for instance,  $v - M$  vs  $M - y$  with  $v - C$  vs  $C - y$ , among other possible combinations. We confirmed such a behavior by plotting the pseudo color diagram  $(C - b) - (b - y)$  vs.  $(v - b) - (b - M)$ . In Figure 4,  $(C - b) - (b - y)$  does not reflect any split between blue and red stars, as expected, while  $(v - b) - (b - M)$  uncovers the different values due to the  $M$  magnitude.

We searched the literature looking for spectral features of early MK-type stars in the wavelength range spanned by the Washington  $M$  passband, and found that the  $H\beta$  emission line is a common feature of Be rotators (see, e.g. Miroshnichenko et al. 2000). According to Fang et al. (2018),  $H\beta$ ,  $H\alpha$ , and Ca II K emission lines are seen in stars spanning a range of mass and rotation in open clusters as a consequence of their chromospheric activity. They also found that  $H\beta$  and  $H\alpha$  emissions are correlated.

At this point, we interpret that fainter and brighter  $M$  magnitudes, responsible of the split between blue and red stars in Figures 1, 3, and 4, correspond to stars with fainter and stronger  $H\beta$  emission lines, which in turn, refers to slow and fast rotators (Dmitriev et al. 2019). Furthermore, the difference derived between  $M$  and  $T_1$  magnitudes of blue and red stars ( $-0.26 \pm 0.07$  mag) confirms the correlation found by Fang et al. (2018) between the  $H\beta$  and  $H\alpha$  emissions in open clusters. The contribution of  $H\beta$  to the  $M$  magnitudes explains the eMSTO observed by Piatti & Cole (2017) in the  $M$  vs.  $C - M$  CMD (their figure 4), similarly as  $H\alpha$  contributes to the  $T_1$  magnitude in the  $T_1$  vs.  $C - T_1$  CMD. This outcome shows that the eMSTO in the CMD of NGC 1971 is observed whenever passbands with Be emission line contributions are used. As far as we are aware, this is the first time  $H\beta$  emissions satisfactorily explain the existence of eMSTOs in young clusters. Nevertheless, further spectroscopic confirmation is highly desired without a doubt. The present outcome opens new possibilities of studying eMSTOs from observational and theoretical perspectives, by using a larger number

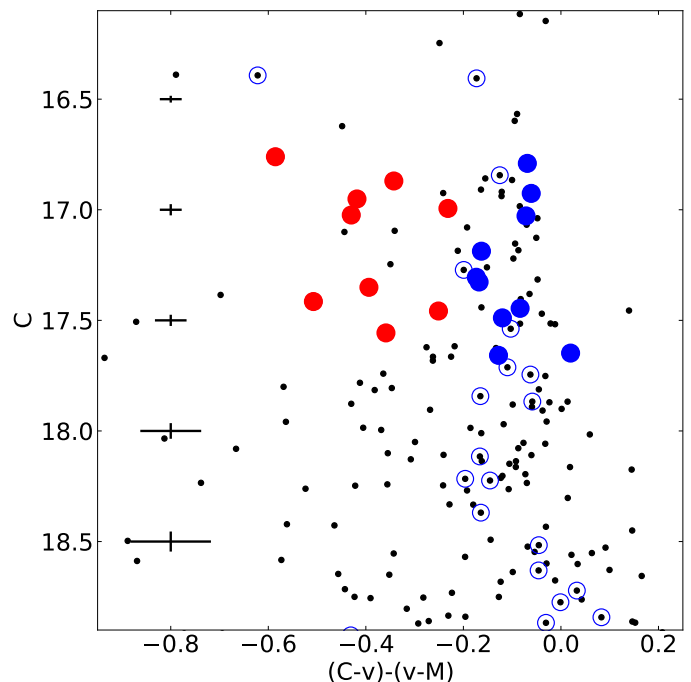


**Fig. 1.** CMD for all the stars measured in the field of NGC 1971 (black dots). Blue and red filled circles represent stars with membership probabilities  $P \geq 75\%$  in the Washington and Strömgren data sets, respectively, and located nearly covering the cluster eMSTO ( $16.7 < C$  (mag)  $< 17.7$ ). Open symbols represent all the stars with  $P \geq 50\%$ .

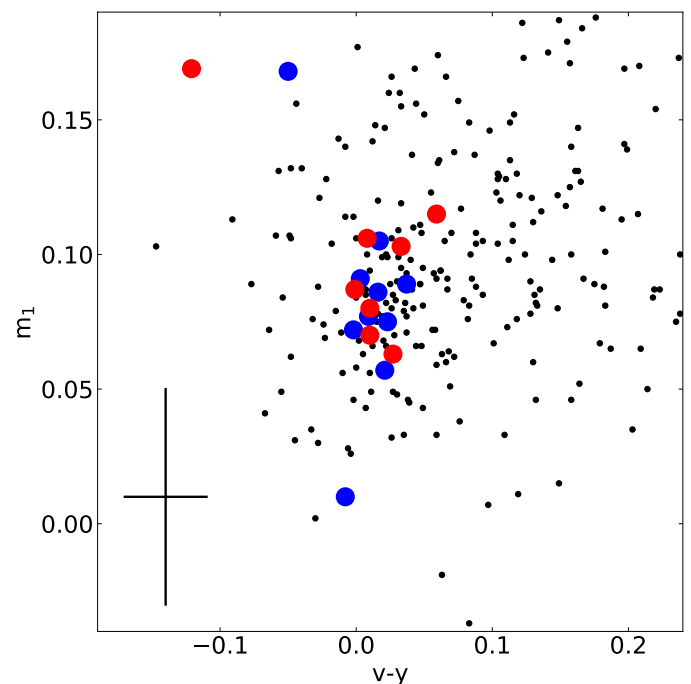


**Fig. 2.** Two-color diagram for stars measured in the field of NGC 1971. Symbols as in Figure 1. Typical error bars for stars represented by blue and red filled circles are also shown.

of photometric systems with passbands centered on Be features, and by improving theoretical isochrones with rotation effects that widen the range of rotation velocities considered.

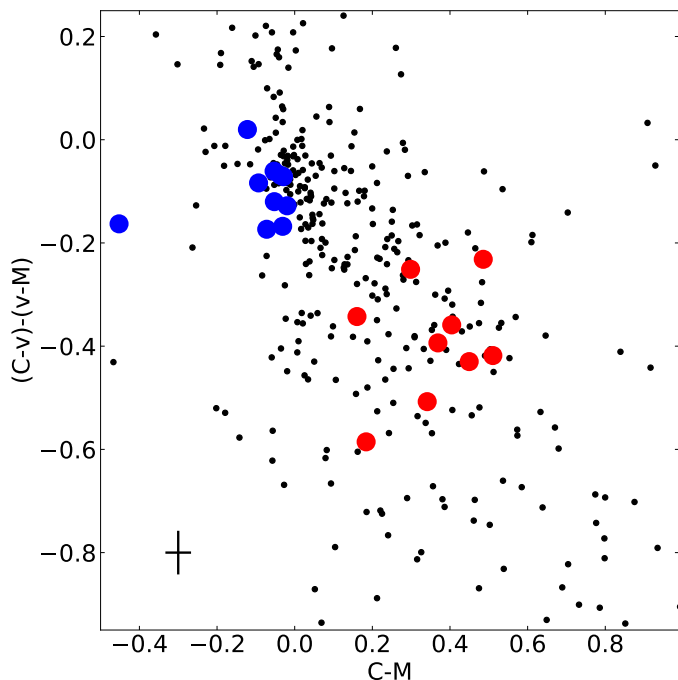


**Fig. 3.** Two-color diagram for stars measured in the field of NGC 1971. Symbols as in Figure 1. Typical error bars for stars represented by blue and red filled circles are also shown.

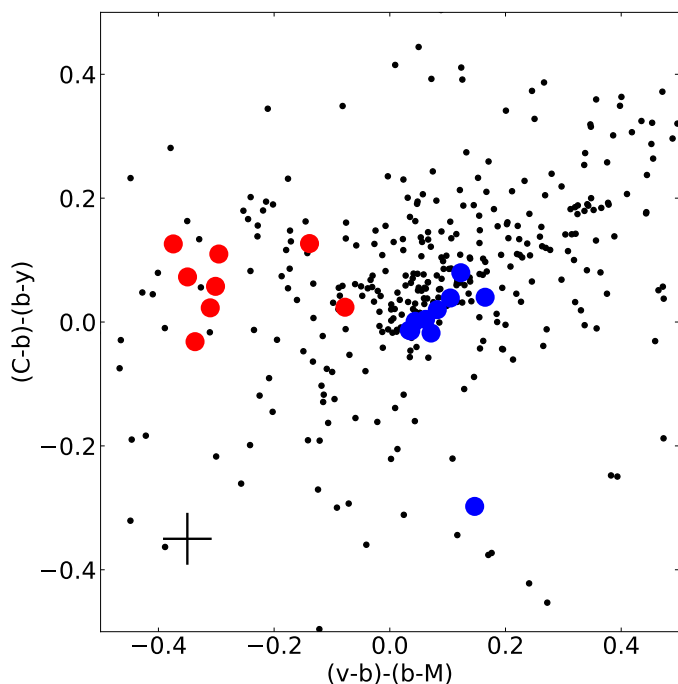


**Fig. 4.** Two-color diagram for stars measured in the field of NGC 1971. Symbols as in Figure 1. Typical error bars for stars represented by blue and red filled circles are also shown.

#### 4. Conclusions

The origin about the existence of eMSTOs in young star clusters is still under debate. During the last years, it has been reached the general idea that neither a real age spread nor stellar evolutionary effects alone explain the observed broadness of the upper part of cluster MSs (Goudfrooij et al. 2017, 2018; Gossage et al. 2019; Li et al. 2020). Moreover, some star clusters do not

seem to exhibit any eMSTO (de Juan Ovelar et al. 2020). In this context, the noticeable large age spread found for NGC 1971 by Piatti & Cole (2017), which resulted to be similar to the cluster age ( $\sim 160$  Myr), caught our attention.

We made use of publicly available and yet not exploited Strömgren *vby* images centered on the cluster, obtained with the SOAR SOI, to search for additional clues about the noticeable eMSTO of NGC 1971. The accurate Strömgren photometry obtained, alongside with the published Washington photometry, allowed us to explore the nature of the broadness at the upper part of the cluster MS observed by Piatti & Cole (2017). During the analysis, we constrained the sample of stars to those with assigned membership probabilities  $P \geq 75\%$  in both photometric data sets, separately. The selected sample consists in 18 stars distributed from the top of the cluster MS down to one magnitude underneath, and spans the range of eMSTO colors.

From an appropriate combination of Washington and Strömgren magnitudes we built different pseudo colors and found that: i) the selected stars can be split into two groups of stars (called 'blue' and 'red'), with 9 stars each; ii) the cluster does not seem to show inhomogeneities of light and heavy-element abundances. On the contrary, both groups of selected stars resembles a single stellar population with an homogeneous chemical abundance level; iii) Blue and red stars are clearly separated only when the Washington  $M$  magnitudes are involved, so that the  $M$  magnitudes are responsible of the appearance of the eMSTO. The spectral region covered by the  $M$  passband comprises  $H\beta$  which, in emission, is a common feature of Be stars. Therefore, we speculate with the possibility that Be stars populate the redder group of stars, in very good agreement with previous findings of eMSTOs in young clusters (e.g. Bastian et al. 2017). Particularly, the present outcome reinforces the suggestion that  $H\alpha$  emissions of Be stars could have contributed to the  $T_1$  magnitudes in (Piatti & Cole 2017), and hence to the detection of an eMSTO. In this work, we confirmed such a possibility from the tight correlation between  $M$  and  $T_1$  magnitudes, as is also shown between  $H\beta$  and  $H\alpha$  emissions of Be stars in open clusters.

I thank the referee for the thorough reading of the manuscript and the suggestions to improve it.

#### References

- Bastian, N., Cabrera-Ziri, I., Niederhofer, F., et al. 2017, *MNRAS*, 465, 4795
- Calamida, A., Bono, G., Stetson, P. B., et al. 2007, *ApJ*, 670, 400
- Canterna, R. 1976, *AJ*, 81, 228
- Cordoni, G., Milone, A. P., Marino, A. F., et al. 2018, *ApJ*, 869, 139
- Crawford, D. L. & Mandwewala, N. 1976, *PASP*, 88, 917
- Cummings, J. D., Geisler, D., & Villanova, S. 2017, *AJ*, 153, 192
- D'Antona, F., Milone, A. P., Tailo, M., et al. 2017, *Nature Astronomy*, 1, 0186
- de Juan Ovelar, M., Gossage, S., Kamann, S., et al. 2020, *MNRAS*, 491, 2129
- Dieball, A. & Grebel, E. K. 2000, *A&A*, 358, 897
- Dmitriev, D. V., Grinin, V. P., & Katysheva, N. A. 2019, *Astronomy Letters*, 45, 371
- Dupree, A. K., Dotter, A., Johnson, C. I., et al. 2017, *ApJ*, 846, L1
- Fang, X.-S., Zhao, G., Zhao, J.-K., & Bharat Kumar, Y. 2018, *MNRAS*, 476, 908
- Gaia Collaboration, Brown, A. G. A., Vallenari, A., et al. 2018, *A&A*, 616, A1
- Gaia Collaboration, Prusti, T., de Bruijne, J. H. J., et al. 2016, *A&A*, 595, A1
- Gossage, S., Conroy, C., Dotter, A., et al. 2019, *arXiv e-prints*, arXiv:1907.11251
- Goudfrooij, P., Girardi, L., Bellini, A., et al. 2018, *ApJ*, 864, L3
- Goudfrooij, P., Girardi, L., & Correnti, M. 2017, *ApJ*, 846, 22
- Hauck, B. & Mermilliod, M. 1998, *A&AS*, 129, 431
- Li, Z., Chen, J., Zhang, S., Deng, Y., & Zhao, W. 2020, *Ap&SS*, 365, 134
- Lim, D., Hong, S., & Lee, Y.-W. 2017, *ApJ*, 844, 14
- Marino, A. F., Milone, A. P., Casagrande, L., et al. 2018a, *ApJ*, 863, L33
- Marino, A. F., Milone, A. P., Renzini, A., et al. 2019, *MNRAS*, 487, 3815
- Marino, A. F., Przybilla, N., Milone, A. P., et al. 2018b, *AJ*, 156, 116
- Marino, A. F., Villanova, S., Piotto, G., et al. 2008, *A&A*, 490, 625
- Milone, A. P., Marino, A. F., Di Criscienzo, M., et al. 2018, *MNRAS*, 477, 2640
- Milone, A. P., Piotto, G., Renzini, A., et al. 2017, *MNRAS*, 464, 3636

- Miroshnichenko, A. S., Chentsov, E. L., Klochkova, V. G., et al. 2000, *A&AS*, 147, 5
- Monelli, M., Milone, A. P., Stetson, P. B., et al. 2013, *MNRAS*, 431, 2126
- Paunzen, E. 2015, *A&A*, 580, A23
- Piatti, A. E. 2018, ArXiv e-prints [arXiv:1809.08123]
- Piatti, A. E. 2020, arXiv e-prints, arXiv:2008.05270
- Piatti, A. E. & Bailin, J. 2019, *AJ*, 157, 49
- Piatti, A. E. & Bica, E. 2012, *MNRAS*, 425, 3085
- Piatti, A. E. & Cole, A. 2017, *MNRAS*, 470, L77
- Piatti, A. E. & Koch, A. 2018, *ApJ*, 867, 8
- Piatti, A. E., Pietrzyński, G., Narloch, W., Górski, M., & Graczyk, D. 2019, *MNRAS*, 483, 4766
- Sbordone, L., Bonifacio, P., Caffau, E., et al. 2010, *A&A*, 522, A26
- Stetson, P. B., Davis, L. E., & Crabtree, D. R. 1990, in *Astronomical Society of the Pacific Conference Series*, Vol. 8, *CCDs in astronomy*, ed. G. H. Jacoby, 289–304
- Yong, D., Meléndez, J., Cunha, K., et al. 2008, *ApJ*, 689, 1020